Diffusion of Xylene Isomers in the MIL-47(V) MOF Material: A Synergic Combination of Computational and Experimental Tools

ARTICLE *in* THE JOURNAL OF PHYSICAL CHEMISTRY C · MARCH 2013

Impact Factor: 4.77 · DOI: 10.1021/jp400507w

THE JOURNAL OF PHYSICAL CHEMISTRY C

Article

pubs.acs.org/JPCC

Diffusion of Xylene Isomers in the MIL-47(V) MOF Material: A Synergic Combination of Computational and Experimental Tools

S. Rives,[†,‡] H. Jobic,*[,‡] D. I. Kolokolov,[§] A. A. Gabrienko,[§] A. G. Stepanov,[§] Y. Ke,[†] B. Frick,[∥] T. Devic,[⊥] G. Férey,[⊥] and G. Maurin*[,†]

[†]Institut Charles Gerhardt Montpellier, UMR 5253 CNRS, UM2, UM1, ENSCM, Université Montpellier 2, Pl. E. Bataillon, 34095 Montpellier Cedex 05, France

[‡]Institut de Recherches sur la Catalyse et l'Environnement de Lyon, Université de Lyon 1, CNRS, 2. Av. A. Einstein, 69626 Villeurbanne, France

[§]Boreskov Institute of Catalysis, Siberian Branch of Russian Academy of Sciences, Prospekt Akademika Lavrentieva 5, Novosibirsk 630090, Russia

[∥]Institut Laue Langevin, BP 156, 38042 Grenoble, France

[⊥]Institut Lavoisier, UMR CNRS 8180, Université de Versailles Saint-Quentin-en-Yvelines, 45 avenue des Etats-Unis, 78035 Versailles cedex, France

ABSTRACT: The dynamics of xylene isomers in the metal−organic framework MIL-47(V) has been investigated by combining molecular dynamics (MD) simulations and experimental tools including quasi-elastic neutron scattering (QENS) and deuterium nuclear magnetic resonance (^{2}H NMR).The experimental and simulated self-diffusion coefficients (D_s) values for each single component isomer are in reasonable agreement in the whole range of temperatures. More interestingly, the simulations predict a nonmonotonous evolution of D_s with the temperature for all xylenes. Such an unusual trend is experimentally confirmed for *p*-xylene. Two distinct diffusion regimes are elucidated at the microscopic level: a low-temperature regime where the xylene molecules are close to the MIL-47(V) pore wall with a high activation energy barrier for the diffusion and a high-temperature regime where the xylene molecules are mainly located in the center of the channel associated with a lower activation energy for the diffusion. This dynamic behavior remains also true whatever the degree of pore filling. It has been further shown that the diffusivity is only slightly affected when one compares the case of xylenes in single component and in mixture. ^{2}H NMR experiments enlighten that packing effects and guest−guest interactions are crucial when considering the dynamics of confined xylenes in MIL-47(V).

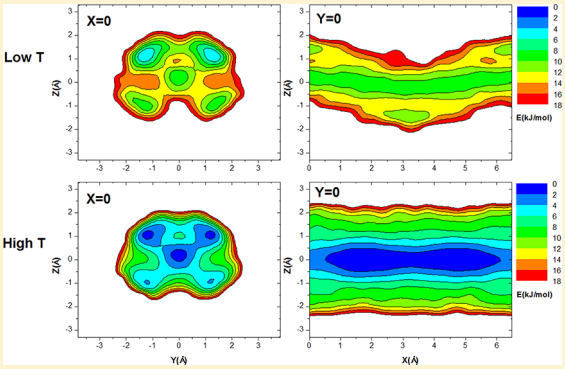

INTRODUCTION

Xylenes isomers that mainly emanate from byproducts of petroleum refining are extensively employed in a broad spectrum of applications, as organic solvent and thinner in the rubber, painting, and leather industries. As single isomers, they are predominantly used as precursors for the preparation of phthalate ester plasticizers and components of polymeric fibers and films.[1]

The separation of the most valuable feedstock *p*-xylene from the others *o*- and *m*-isomers is one of the challenging issues in the chemical industry because of the similarity of their boiling points (411.37, 412.12, and 417.41 K for *p*-, *m*-, and *o*-xylene, respectively). While a fractional crystallization procedure[2−4] based on the different isomers freezing points (286.26, 225.13, and 247.82 K for *p*-, *m*-, and *o*-xylene, respectively) can be envisaged, the PAREX process involving the use of a packed bed adsorption column in a simulated moving bed is most often favored for its larger production rate, lower cost, and higher selectivity.[5−13] The efficiency of such a physisorption-based strategy mainly relies on the choice of a highly selective adsorbent for the mixture of interest among the conventional class of porous materials including zeolites (MFI, faujasites X and Y) exchanged by different extraframework cations (Ba^{2+}, Na^+, or K^+),[14−22] carbons,[23,24] and polymer materials.[25]

More recently, the emerging hybrid porous coordination polymers (PCPs), also called MOFs (metal−organic frameworks), built up from inorganic subnetworks (clusters, chains or layers) connected to polydendate organic molecules (phosphonates, carboxylates, azolates)[26] have shown great promises for the selective adsorption of diverse molecules[27−33] due to their highly chemical and topological richness. The presence of organic moieties within their pore walls are further

Received: January 16, 2013
Revised: March 4, 2013
Published: March 6, 2013

expected to give rise to additional interactions (van der Waals, $\pi-\pi$) with organic guest molecules that can favor the separation of hydrocarbons and aromatics. Indeed, a few MOF materials have already demonstrated their abilities to selectively adsorb xylene isomers.[34−45] Among them, the microporous MIL-47(V) (MIL stands for Materials of Institut Lavoisier), which is built up from chains corner-sharing $V^{4+}O_6$ octahedra interconnected by terephthalate groups defining a 1D type diamond-shaped pore system, has been shown to be *p*-xylene selective for a mixture of the three isomers.[46−48] These findings based on breakthrough and chromatographic experiments were further completed by a computational study by Castillo et al.,[49] which predicted by means of grand canonical Monte Carlo simulations that the *o*-xylene/*m*-xylene thermodynamic selectivity should be even larger than the *p*-xylene/*m*-xylene one, in contradiction with the experimental trend. The authors assumed that this deviation may be due to diffusion limitations. More recently, Ghysels et al.[50] have conducted a careful analysis of the xylene/MIL-47(V) framework and the xylene/xylene interactions using high quality density functional theory (DFT) calculations. They suggested that as the interaction energies are very similar for all isomers, the separation properties of MIL-47(V) should be mainly driven by entropic effects.

Indeed, it is of interest to explore the dynamics of the confined xylene molecules for gaining preliminary fundamental insight into the mechanism in play that could govern such a separation process. As far as we know, neither experimental nor simulated data are reported yet on the mobility of the xylene isomers in both single and mixture components in such a MOF. In light of this lack of available literature, much effort is still required to get a complete picture of the adsorption/separation processes. Quasi-elastic neutron scattering (QENS) measurements have been widely combined with molecular dynamics (MD) in recent years, sometimes with ^{2}H NMR, to successfully address the molecular motions of pure and mixed fluids (hydrogen, benzene, short and long chain linear alkanes, carbon dioxide, water) confined in diverse MOFs.[51−61] In the present work, a joint QENS-MD approach is undertaken to fully characterize the dynamics of each single component xylene isomer and the binary *p*-/*m*-xylene mixture in the MIL47-(V) for a wide range of temperatures (200−500 K). This effort is completed by solid-state ^{2}H NMR measurements in order to probe the rotational motions of the xylenes occurring on longer time scales.

METHODOLOGY

Materials. The MIL-47(V) samples were synthesized and activated using published procedures[63] with hydrogenated or deuterated terephthalic acid as reactant for the NMR or QENS experiments, respectively. The activation is performed in order to ensure that the dynamics of the xylene molecules is not affected by any remaining solvent.

Quasi-Elastic Neutron Scattering. The neutron experiments were performed at the Institut Laue-Langevin, Grenoble, France, using the backscattering spectrometer IN16. The incident neutron energy was 2.08 meV (6.271 Å), using a Si(111) monochromator. Spectra were recorded at different scattering angles, corresponding to wavevector transfers, *Q*, ranging from 0.19 to 1.9 Å^{-1}. Quasi-elastic spectra were obtained by applying a Doppler shift to the incident neutrons through a movement of the monochromator. The energy transfer was then analyzed in a window of ±14.5 μeV, using unpolished Si(111) crystals. The energy resolution, measured with a vanadium standard or with the empty MIL-47(V), could be fitted by a Gaussian function, with a fwhm of the order of 1 μeV, depending on *Q*.

Deuterated MIL-47(V) was used for the neutron experiment to decrease the scattering from the organic linkers. The MOF was activated at 473 K under vacuum (10^{-2} Pa) prior to adsorption experiments. Several samples, containing various amounts of xylene isomers, were prepared. The lowest concentration for each xylene was 1 molecule per uc (unit cell, which correspond to 1 molecule per four linkers). *p*-Xylene was also studied at a higher concentration, 2.5 molecules/uc, and a mixture of *p*- and *m*-xylene (80−20%) was also considered at the same total concentration. In the mixture, hydrogenated *p*-xylene and perdeuterated *m*-xylene were used, the signal coming essentially from *p*-xylene due to the larger cross section of hydrogen (to get a reasonable signal, a larger proportion of *p*-xylene was selected). After equilibration at 423 K for several hours, the samples were transferred inside a glovebox into cylindrical aluminum containers of annular geometry. The scattering from a cell containing the same amount of activated MIL-47(V) was subtracted from the QENS spectra recorded with the loaded samples. The containers were placed in a cryofurnace, so that measurements could be made in the temperature range 200−500 K.

Nuclear Magnetic Resonance. ^{2}H NMR experiments were performed at 61.432 MHz on a Bruker Avance-400 spectrometer, using a high-power probe with 5 mm horizontal solenoid coil. V^{4+} centers in the MIL-47(V) structure are paramagnetic (S = 1/2) which may influence the ^{2}H NMR spectrum by large chemical shifts and fast relaxation of the nuclear spin.[62] To compensate these effects and correctly refocus the ^{2}H NMR spectrum an Exorcycled quadrupole-echo sequence was used,[64] ($90_X-\tau_1-90_Y-\tau_2-$Acq$-t$), where τ_1 = 20 μs, τ_2 = 22 μs, and t is a repetition time for the sequence during the accumulation of the NMR signal. The duration of the 90° pulses was 1.8−2.2 μs. To capture all dynamical features of the system, the measurements were performed over a broad temperature range, from 123 to 423 K. Perdeuterated xylenes with 98% ^{2}H isotopic enrichment was purchased and used without further purification. We used also *p*-xylene, selectively deuterated on the aromatic ring, to remove the contribution from the methyl groups.

To prepare the sample, 0.35 g of hydrogenated MIL-47(V) was loaded in a 5 mm (o.d.) glass tube, connected to a vacuum system. The sample was heated at 473 K for 12 h in air and for 24 h under a vacuum of 10^{-3} Pa. After cooling back to room temperature, the material was loaded with a required amount of molecules of a given xylene isomer per unit cell and sealed off. The adsorption was performed from xylene vapor with the MOF powder kept at the temperature of liquid nitrogen. The sealed sample was equilibrated at 373 K for 10 h.

Molecular Dynamics Simulations. The crystal structure of the MIL-47(V) material was built using the atomic coordinates previously derived from X-ray diffraction data.[63] The framework was first maintained rigid during the MD simulations for all xylene isomers. This assumption is based on the conclusions drawn from previous *in situ* X-ray[46,65] and neutron[54,66] diffraction measurements which have shown that the MIL-47(V) structure does not undergo any significant modification upon adsorption of *n*-alkanes or benzene. However, as recent ^{2}H NMR[66] spectroscopy evidenced that the phenyl rings of the MIL-47(V) can execute π flips around

dx.doi.org/10.1021/jp400507w | J. Phys. Chem. C 2013, 117, 6293−6302

their symmetry axis, a specific force field for treating the MOF framework that we recently derived[67] has been also considered in the MD simulations to estimate the impact of the flexibility of the framework on the diffusivities of the confined xylenes.

The partial charges carried by each atom of the framework were taken from previous DFT calculations[68] while the Lennard-Jones (LJ) potential parameters of the inorganic node of MIL-47(V) (corresponding to the metal center with the surrounding oxygen atoms) and the organic part were taken from the UFF[69] and the Dreiding force field,[70] respectively.

The xylene molecules were microscopically described by a point-charge model as follows. Following our previous work on the benzene confined in the same host material,[54] the aromatic ring is treated explicitly by the TraPPE-EH force field[71] as rigid. The methyl group is further modeled by a single interacting site as defined by the TraPPE-UA force field,[72] its flexible character being described by the intraframework potential parameters reported by Oie et al.[73] The atomic charges for the carbon and the hydrogen atoms of the phenyl ring are taken as −0.095 and 0.095, respectively,[54] while the charges of the methyl group are set to 0.095. Indeed, the xylenes/MIL-47(V) interactions include a Coulombic contribution and a van der Waals term, the LJ crossing parameters being obtained using Lorentz−Berthelot mixing rules.

The MD simulations were further realized using the DL_POLY package[74] in the *NVT* ensemble coupled with the Beredsen thermostat[75] while for testing the impact of the MIL47-(V) flexibility, complementary calculations were run in the *NσT* Hoover thermostat/barostat which allows size and shape changes of the framework. The optimal relaxation times for the thermostat and the barostat were 1 and 5 ps, respectively, which is a compromise between the simulation time and energy stability. The simulation box consisted of 48 unit cell (12 × 2 × 2) loaded with 48 and 120 xylene molecules to mimic the experimental loading. The calculations were run at five different temperatures from 200 to 500 K, each for 10^7 steps (i.e., 10 ns in total) with a time step of 1 fs, following 1 ns of equilibration. A cutoff radius of 12 Å was applied to all the LJ interactions, and the long-range electrostatic interactions were handled using the Ewald summation technique.

From the mean-square displacement (MSD) curves averaged over multiple time origins and three different MD trajectories, the self-diffusivities (D_s) for xylene molecules were evaluated based on the Einstein equation.[75] The orientation into the MIL-47(V) channel of the in-plane and out-of-plane C_2 axes of the xylenes molecules have also been analyzed from the MD trajectories. The in-plane C_2 axis corresponds for *p*-xylene to the vector joining two methyl groups while the out-of-plane C_2 axis is the axis perpendicular to the phenyl ring. The orientation of these axes within the 1D channel of MIL47-(V) is defined by two angles: the angle between the C_2 axis and the channel direction (here the *X*-axis) and the direction along the C_2 axis in a plane perpendicular to the channel (here the *XZ*-plane), the positions 0°, ±90°, and 180° corresponding to the lozenge pore corners. 2D free energy maps and isosurfaces were also extracted from the MD trajectories using the histogram sampling method previously reported by Beerdsen et al.[76]

RESULTS

For a concentration of 1 xylene molecule/uc, one first experimentally observes that the temperature dependence of the diffusivity of *p*-xylene significantly differs from the two other isomers. The QENS spectrum shown in Figure 1a corresponds to *p*-xylene at 250 K. The broadening is very small, at the limit of the resolution function, indicating a low mobility.

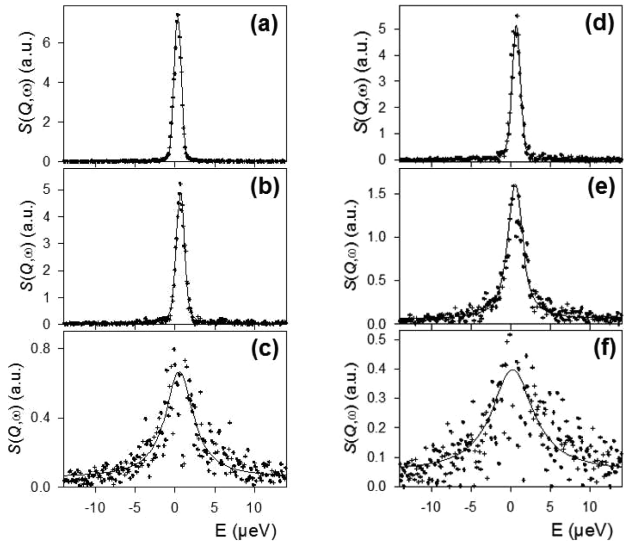

Figure 1. Comparison between experimental (crosses) and calculated (solid lines) spectra obtained for Q = 0.29 Å^{-1} for 1 *p*-xylene/uc in MIL-47(V) at different temperatures: (a) 250, (b) 280, and (c) 300 K and for 1 *m*-xylene/uc; (d) 210, (e) 250, and (f) 300 K.

The experimental data are fitted with a translational scattering function convoluted with the instrumental resolution. The rotational motions of the methyl groups and of the phenyl ring occur at much shorter time scales[77] so that the quasi-elastic due to these motions will look flat on our time scale. At 280 K, the broadening slightly increases (Figure 1b), but it becomes really large only at 300 K (Figure 1c), suggesting a transition between these two temperatures. This is confirmed by the self-diffusivities computed using a Fickian diffusion model. The values in Figure 2 show a transition around 300 K; one can estimate the activation energy only above 300 K (7 kJ/mol).

On the other hand, *m*-xylene is mobile at 250 K, as shown in Figure 1e. In fact, a diffusion coefficient can be already obtained at 210 K for this molecule (see Figure 1d). The values extracted

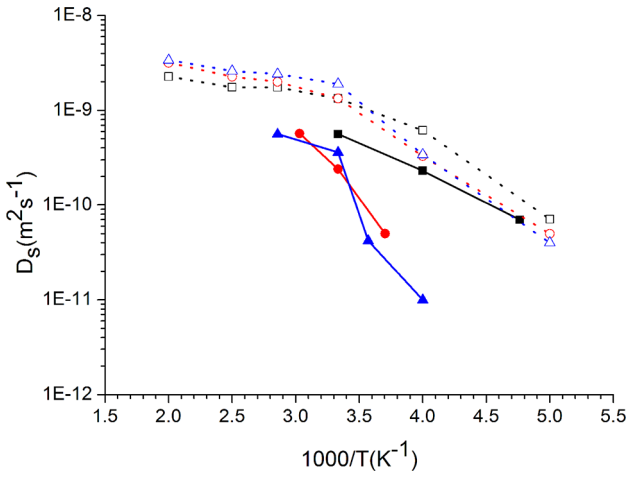

Figure 2. Evolution of the self-diffusion coefficient as a function of temperature for a loading of 1 xylene molecule/uc. Solid line: QENS experiment; dashed line: MD simulation. Squares are for *m*-xylene, circles for *o*-xylene, and triangles for *p*-xylene.

dx.doi.org/10.1021/jp400507w | J. Phys. Chem. C 2013, 117, 6293−6302

in the range 210−300 K are reported in Figure 2, and they follow a simple Arrhenius behavior, with an activation energy of 12 kJ/mol. *o*-Xylene also follows an Arrhenius law, with a higher activation energy, 30 kJ/mol, and it intersects twice the line joining the points obtained for *p*-xylene.

To get microscopic insight into the different diffusion behaviors for *p*-xylene detected by QENS, MD simulations were further conducted for the three individual isomers in a broader range of temperatures from 200 to 500 K. The so-simulated self-diffusion coefficients, which are orientationally averaged values ($D_s = D_{1D}/3$) to be consistent with the QENS data, are reported in Figure 2. These simulations first confirm a nonmonotonous evolution of D_s for *p*-xylene as evidenced by QENS, with a transition between two diffusion regimes also observed at about 300 K, each characterized by a linear evolution of $\ln(D_s) = f(1000/T)$. Moreover, the *o*- and *m*-xylenes are predicted to have a similar unusual D_s profile as *p*-xylene. Such a statement which at first sight seems to be contradictory with the QENS conclusions cannot be totally excluded as the experiments were not performed for temperatures higher than 330 K. Further, the significant change of the simulated activation energies for all xylenes (Table 1) when one

Table 1. Activation Energy Extracted from MD Simulations for Low- and High-Temperature Regimes at a Loading of 1 Xylene Molecule/uc[a]

isomer	E_a (200−300 K)	E_a (300−500 K)
m-xylene	15 [12]	3
o-xylene	16 [30]	5
p-xylene	20	3 [7]

[a]The values reported in brackets are obtained from QENS data.

goes from the low- to high-temperature domain also supports the existence of two distinct diffusion regimes. This different energetic behavior is confirmed by the QENS data when available, the E_a value in the range 300−500 K being significantly smaller than those obtained in the low-temperature domain. The simulated and experimental activation energies in both domains of temperature (Table 1) are in good agreement within a factor of ∼2.

From an experimental standpoint, it has been evidenced that in the low-temperature range the diffusivity of the different isomers follows the sequence D_s(*m*-xylene) > D_s(*o*-xylene) > D_s(*p*-xylene), consistent with the MD simulations. Above 300 K, all the experimental D_s tend to converge toward a very similar value around 6×10^{-9} m^2 s^{-1}. This behavior is well captured by the MD simulations which evidence that in the high-temperature regime *p*-xylene becomes only slightly faster than *m*- and *o*-xylenes. One can notice that this trend follows the evolution of the kinetic diameter of these species (5.85 Å vs 6.80 Å for *p*- and *o*-/*m*-xylene, respectively). However, while the simulated D_s fairly reproduce the experimental values for *m*-xylene, they significantly deviate by about 1 order of magnitude for *o*- and *p*-xylenes. This behavior also holds true when one compares the simulated and experimental activation energies (Table 1), the values for *m*-xylene being much closer than for *o*- and *p*-xylenes.

Complementary MD simulations were conducted using a flexible MIL-47(V) to ensure that the structural relaxation of the host is not at the origin of such a discrepancy. Figure 3 clearly shows that there is only a minor change of the simulated D_s values when one considers the flexibility of the framework,

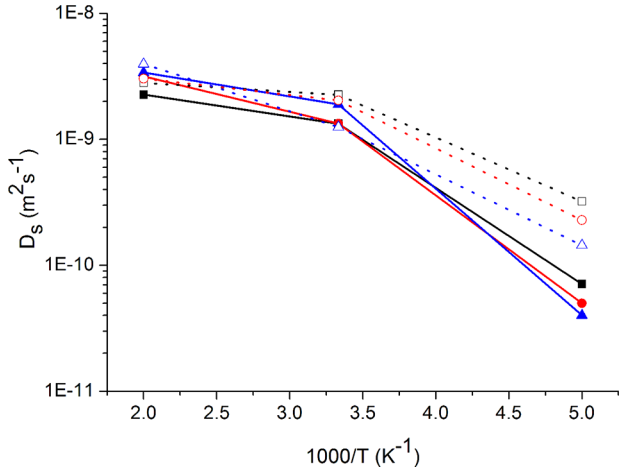

Figure 3. Simulated self-diffusion coefficients for *p*-xylene (triangles), *m*-xylene (circles), and *o*-xylene (square) considering a rigid (straight lines) and a flexible MIL-47(V) framework (dotted lines).

which does not allow a better matching of the experimental data at low temperature for the *o*-/*p*-xylenes. Besides this consideration, the deviation between the experimental and simulated data at low temperature might come from the description of the host/guest interactions implemented in our MD simulations.

A careful analysis of the MD trajectories followed by each isomer has been further undertaken in both ranges of temperatures 200−300 and 300−500 K where the dynamics of the confined species might correspond to two distinct molecular motions mechanisms as previously suspected for the same xylene isomers in the faujasite-type zeolite by Zhai et al.[78] as well as for benzene in IRMOF-1 by Takakura et al.[79]

The 2D free energy maps for all xylene isomers were first derived from their spatial density probabilities through planes either perpendicular or parallel to the tunnel of MIL-47(V). As a typical illustration, Figure 4 which reports the 2D free energy maps for *p*-xylene at 250 and 400 K clearly emphasizes that the most preferential regions are either close to the pore walls near the phenyl ring or mainly located in the middle of the pore.

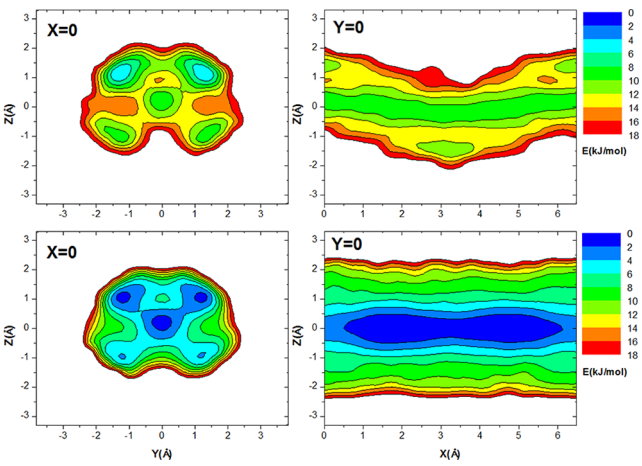

Figure 4. 2D slices of the free-energy map for 1 *p*-xylene/uc; isoline spacing corresponds to 1 kJ/mol. Top: 250 K; bottom: 400 K. Left: slice along the channel direction, Right: slice through the channel direction.

dx.doi.org/10.1021/jp400507w | J. Phys. Chem. C 2013, 117, 6293−6302

One further observes that this central zone becomes even much more favorable at higher temperature (see Table 2).

Table 2. Proportion of *p*-Xylene Present near the Pore Walls and in the Central Region of the Pore for a Loading of 1 *p*-Xylene/uc[a]

temp (K)	proportion of *p*-xylene close to the pore walls (%)	proportion of *p*-xylene in the central region (%)
200	88	<1
250	77	4
300	46	18
400	22	35
500	15	43

[a]The following criteria have been employed to define the position of the xylene center of mass (COM) within the porosity. A molecule is considered to be near the pore wall if the radial position of its COM is at a distance of 1.8 ± 0.3 Å from the pore center. In contrast, if the radial position of its COM is situated at a distance below 1 Å from the center of the pore, the molecule is counted as occupying this central region of the pore.

The minimum-energy pathways for *p*-xylene molecules in the pores can be approximately drawn by following the lower parts of the 2D free energy maps (Figure 4). They are predominantly oriented along the direction of the tunnel confirming a 1D diffusion mechanism for both ranges of temperatures. At 250 K (Figure 4), one can imagine a jump sequence between two consecutive energy pockets situated around the phenyl ring of the pore walls, with a mean jump length of 6.8 Å. At higher temperature, i.e. at 400 K, in addition to such a diffusion-type mechanism, the *p*-xylene predominantly tends to diffuse following a pathway centered on the middle of the pore. A visual inspection of the trajectories unambiguously confirms that in the low-temperature range the *p*-xylene molecules experience a jump-diffusion-type mechanism between basins near the wall along a 2-fold screw axis similarly to benzene in the same material,[54] while at higher temperature the confined species follow a jump-diffusion process along the channel center which requires to cross lower energy barrier. These conclusions hold also true for the two other xylene isomers.

Such distinct diffusion mechanisms are consistent with the evolutions of the xylenes/MIL-47(V) mean interaction energy averaged over the MD runs which are reported in Figure 5. Indeed, one observes that at low temperature the interaction energies reach the highest value in line with a relative strong interaction between the xylenes and the phenyl ring of the pore wall and further decrease when the temperature increases concurrent with a less energetic distribution of the confined species in the middle of the pore. One can further notice that this energy profile shows a slope change in the same range of temperature as the D_s evolution, which suggests that the host/guest interactions mainly rule the dynamics behavior of xylenes. It is also remarkable to observe that when at high temperature this interaction energy remains almost the same for all xylene isomers, it follows that their corresponding D_s converge toward a similar value (Figure 2). Regarding the low-temperature domain, the interaction energy sequence coincides with that of the self-diffusivity; however, the strength of the host/guest interactions which only slightly changes from one xylene to another can explain that their corresponding simulated D_s values are within the same order of magnitude in contrast with the diffusive behavior observed by QENS. Indeed, this

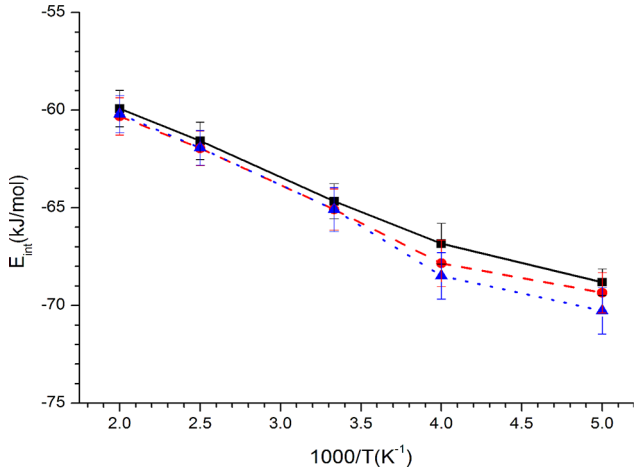

Figure 5. Evolution of the interaction energy between xylene isomers and the MIL-47(V) framework as a function of the temperature, for a loading of 1 molecule/uc: *m*-xylene (black squares), *o*-xylene (red circles), and *p*-xylene (blue triangles).

observation supports that a more accurate description of the host/guest interactions would lead to a more pronounced discrimination of the D_s values in the low-temperature range as suggested above.

In addition, a careful analysis of the configurations generated at high loading leads to the conclusions that the xylene molecules close the pore wall are distributed by pairs with their out-of-plane C_2-axis perpendicular to the channel axis, while when they are present in the middle of the pore they are oriented in such a way to have their out-of-plane C_2-axis parallel to the direction of the tunnel. Typical illustrations are provided in Figure 6 which are consistent with the conclusions drawn from previous studies issued from crystal structure Rietveld refinement,[46] GCMC,[49] and DFT[50] calculations.

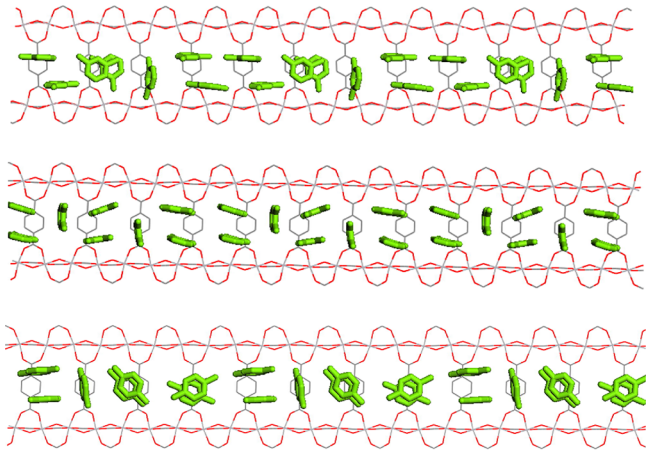

Figure 6. Simulated geometries of the confined xylenes in MIL-47(V) at high loading: *m*-xylene (top), *o*-xylene (middle), and *p*-xylene (bottom).

The impact of the xylenes loading on their D_s values has been further investigated by molecular dynamic simulations (Figure 7), and it was evidenced (i) a D_s decrease when the xylene concentration increases and (ii) again the existence of two diffusion regimes. QENS experiments confirmed that the mobility of the confined molecules is reduced at high loading,

dx.doi.org/10.1021/jp400507w | J. Phys. Chem. C 2013, 117, 6293−6302

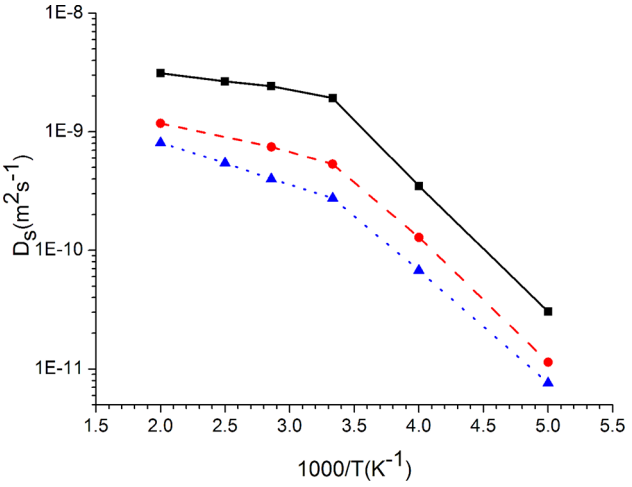

Figure 7. Evolution of the simulated self-diffusion coefficient for *p*-xylene at different loadings as a function of the temperature: 1 molecule/uc (squares), 2 molecules/uc (circles), and 2.5 molecules/uc (triangles).

as shown typically in Figure 8 for *p*-xylene. No broadening could be measured around room temperature, and self-

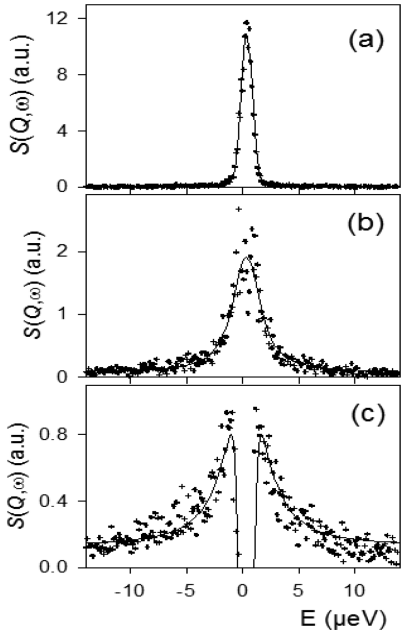

Figure 8. Comparison between experimental (crosses) and calculated (solid lines) spectra obtained for $Q = 0.29$ Å^{-1} for 2.5 *p*-xylenes/uc in MIL-47(V) at different temperatures: (a) 400, (b) 450, and (c) 480 K.

diffusivity coefficients were obtained above 400 K (Figure 9a). The associated activation energy is much higher than at low concentration: 67 kJ/mol for a loading of 2.5 molecules/uc.

As a further step, we also probed the dynamics of the molecules for a same loading of 2.5 molecules/uc in a *p*-/*m*-xylenes (80/20) mixture. One observes in Figure 9a that the self-diffusion coefficients of *p*-xylene obtained by QENS for the mixture are not significantly modified in the high-temperature domain compared to its single-component behavior. However, one can notice that, in the presence of *m*-xylene, *p*-xylene diffuses faster or slightly slower in the low- and high-temperature ranges, respectively, with an E_a of 47 kJ/mol.

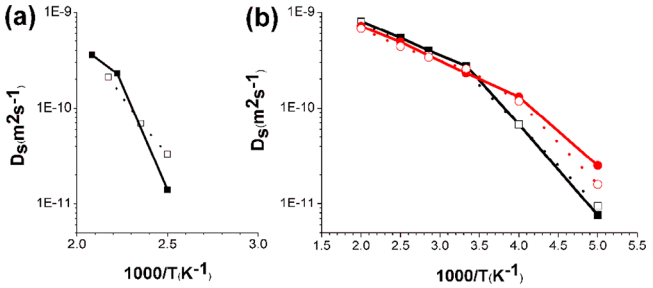

Figure 9. (a) Self-diffusivity for *p*-xylene extracted from QENS in single component at 2.5 *p*-xylenes/uc (solid lines and full symbols) and in binary mixture 2 *p*-xylenes/0.5 *m*-xylene/uc (dotted lines and empty symbols). (b) Simulated self-diffusivity for *p*-xylene (squares) and *m*-xylene (circles) in single component at 2.5 molecules/uc (solid lines and full symbols) and in binary mixtures 2 *p*-xylenes/0.5 *m*-xylene/uc (dotted lines and empty symbols).

In order to deepen understanding the codiffusion mechanism, the self-diffusion coefficients for *p*-xylene and *m*-xylene have been extracted from MD simulations in the binary mixture corresponding to the same composition as that experimentally investigated (Figure 9b). One observes that in the low-temperature region the slowly diffusing *p*-xylene retards the faster *m*-xylene species, which nevertheless diffuses still faster. In contrast in the high domain of temperature, the D_s of both isomers in the mixture are closer together and very similar to the values obtained in single components. This phenomenon has already been observed among others for the diffusion of CO_2/CH_4 mixtures across the channels of MFI zeolites with a significant slowing down of the more mobile CH_4 with concomitant speeding-up of the slowly diffusive CO_2 species.[80] This was explained by an important correlation between the different species diffusing across a 1D channel,[81] which is even more pronounced at high loading. One notice that this dynamic behavior significantly differs with that previously observed in the narrow window UiO-66(Zr) MOF type solid, the slower CO_2 enhancing the mobility of the faster CH_4.[60,61]

Experimentally, this correlation effect explains why at low temperature *p*-xylene diffuses faster in a mixture than in single component and diffuses a bit slower at higher temperature. However, one observes that the transition between the two diffusion regimes mentioned above occurs at a higher temperature than the simulated one.

The orientation of the in-plane and of the out-of-plane C_2-axes of *p*-xylene has been extracted at 300 K from the MD trajectories for the two scenarii where the molecules are (i) close to the wall and (ii) localized in the center of the pore. For the first situation, their out-of-plane C_2-axes are almost perpendicular to the tunnel (Figure 10b) pointing toward the opposite wall while their in-plane C_2-axes form with the channel axis two distinct distributions of angles centered on 46° and 134° (Figure 10a) with an orientation along the wall. Indeed, such well-localized orientations of *p*-xylene suggest that these molecules undergo anisotropic rotations about in-plane and out-of-plane axes. This orientational behavior significantly differs with that for *p*-xylene present in the central zone of the pore. While the in-plane C_2-axes of the molecules form with the direction of the channel two distributions of angles centered on 50° and 130° (Figure 10a) similarly to that mentioned above for the first case, but pointing now toward the corners of the pore, the orientations of the out-of-plane C_2-axes are more homogeneously distributed leading to angles with the channel

dx.doi.org/10.1021/jp400507w | J. Phys. Chem. C 2013, 117, 6293−6302

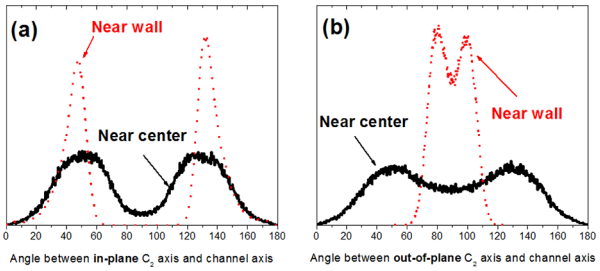

Figure 10. Orientation of the *p*-xylene molecule in the MIL-47(V) channel when present near the wall (dotted lines) or in the central region of the pore (straight lines) for a loading of 1 molecule/uc at 300 K.

axis varying in a broad domain [30°−150°] (Figure 10b). Indeed in this central region, the less localized orientation of the out-of-plane axis tends to prove that the *p*-xylene molecules experience isotropic rotation about their in-plane axes.

To obtain information complementary to the QENS and MD techniques, we have performed the monitoring of the xylenes isomers mobility in the MIL-47(V) channels at low and high concentrations by ^{2}H NMR in a broad temperature range.

The evolution of the ^{2}H NMR spectra line shape with temperature for both *p*- and *m*-xylenes allows us to compare the rotational dynamics of the two isomers adsorbed into hydrogenated MIL-47(V) channels at low loading (see Figure 11). There are two signals in the spectra: one arising from the

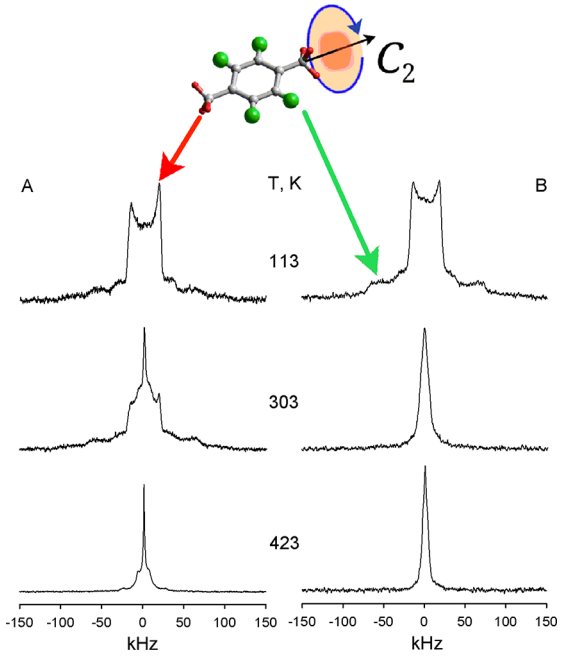

Figure 11. Experimental ^{2}H NMR spectra line shape evolution for the fully deuterated *p*-xylene (A) and *m*-xylene (B) in MIL-47(V) over a wide temperature range (0.6 molecule/uc).

deuterium atoms in the benzene rings and another one from the deuterons in the methyl groups. At 113 K, each spectrum is composed by a broad ($Q \sim 180$ kHz, $\eta \sim 0$) and a narrow ($Q \sim 60$ kHz, $\eta \sim 0$) Pake-powder doublets. The less intense broad one is attributed to a rigid benzene ring, while the narrow one to a rapidly rotating methyl group around the C−C bond.[82] This indicates that at 113 K both isomers are completely immobile on the ^{2}H NMR time scale.

At 303 K, the line shapes of the two isomers differ dramatically from each other: *m*-xylene has its broad anisotropic signal almost completely averaged, with a single central line remaining, while the line shape for *p*-xylene remains generally unchanged with only a relatively weak isotropic peak appearing in the central part of the spectrum. A single line shape of Lorentzian type in the central part of the *m*-xylene spectrum indicates that a highly symmetric rotation is present.[83] This points to a (pseudo)isotropic rotation of *m*-xylene. In the case of *p*-xylene, one can state that its motion is still slow and underdeveloped with a characteristic time $\tau_C \sim 10^{-5}$ s. On the other hand, the motion exhibited by *m*-xylene is already found in the fast limit regime, i.e., with a characteristic time $\tau_C < 10^{-6}$ s.[84,85] This comparison demonstrates that *m*-xylene moves 1 order of magnitude faster that *p*-xylene around 300 K, in agreement with the results obtained by QENS.

At higher temperatures, the line shape evolution supports the higher rotational barrier for the *p*-isomer. The *p*-xylene spectrum starts to be dominated by an isotropic signal only at ≈423 K, while the *m*-xylene line shape is governed by a narrowing Lorentzian pattern already at 303 K. Hence, the NMR experiment supports the higher mobility of *m*-xylene at low loadings.

In order to better understand the confinement effect caused by the MIL-47(V) channels on *p*-xylene, to characterize its dynamical freedom and to show the packing effect and the influence of the meta isomer, we followed the *p*-xylene dynamics as a single adsorbate at low (0.6 molecule/uc) and high (3.4 molecules/uc) loadings and in a mixture (1.7 +1.7 molecules/uc) with the nondeuterated *m*-isomer (the *p*-xylene under investigation was selectively deuterated in the aromatic ring).

Figure 12 shows the evolution of the ^{2}H NMR spectrum line shape with temperature for all three cases. First, we consider

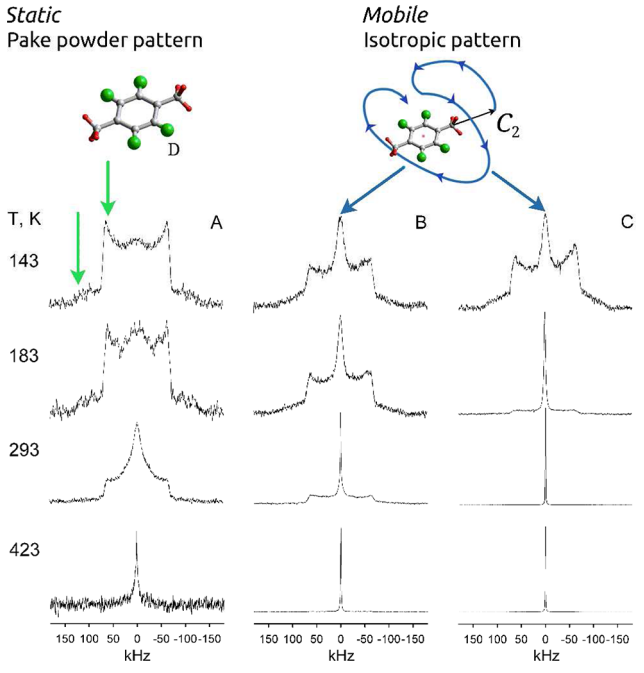

Figure 12. Experimental ^{2}H NMR lines shapes for *p*-xylene, selectively deuterated in the aromatic ring, confined into MIL-47(V): (A) 0.6 molecule/uc; (B) 3.4 molecules/uc; (C) mixture of deuterated *p*-xylene and undeuterated *m*-xylene (1.7 + 1.7 molecules/uc).

dx.doi.org/10.1021/jp400507w | J. Phys. Chem. C 2013, 117, 6293−6302

results for a low loading, 0.6 molecule/uc (Figure 12A). In this case the dynamics is considered to be mainly influenced by the guest−host interaction. Within the monitored temperature interval, the spectral line shape continuously evolves from totally static on the ^{2}H NMR time scale (T < 153 K) to a single isotropic-like line shape with quadrupolar constant (Q ∼ 180 kHz) completely averaged by motion (T > 423 K). The intermediate line shapes show that *p*-xylene exhibits a rather complex mobility characterized by a high activation barrier, since at 303 K the broad Pake-powder pattern of deuterons from the aromatic ring remain mostly unaveraged by the molecular motion. In fact, the central isotropic line starts to dominate the total line shape only above 373 K, while in accordance with Figure 11 and with QENS data, the reorientations remain slow below room temperature.

Further, we focused on *p*-xylene adsorbed into MIL-47(V) channels at loadings close to saturation, i.e., 3.4 molecules/uc. The experimental spectra for pure *p*-xylene at high loading are given in Figure 12B. Below 143 K, the spectrum is again represented by immobile molecules. Above this temperature the spectrum is composed by the static signal and a central isotropic line whose intensity increases with a rise in temperature. The broad anisotropic signal is completely averaged by the molecular motion above 400 K. If we compare the relative intensities of the isotropic and anisotropic signals (the ratio between the two is proportional to the percentage of molecules involved in fast isotropic motion), the difference between the low and the high loadings becomes evident. At high loading, the fast isotropic motion dominates already at ∼300 K.

In the 50/50 mixture of *p*- and *m*-xylene, the influence of *m*-xylene on the *p*-isomer mobility can be revealed. Experimental results given in Figure 12C show that the line shape evolution follows the same trend as the one described for pure *p*-xylene (Figure 12B). The difference in the rotational rates is however more profound: in the mixture with the *m*-isomer, *p*-xylene is already very mobile at 183 K, i.e., by 100 K slower when compared with the high loading of pure *p*-xylene. This means that the presence of the more mobile *m*-isomer induces a higher mobility for *p*-xylene. This experimental evidence agrees with the QENS and MD results and emphasizes the importance of the guest−guest interactions when considering the dynamics of mixed species in confinement.

CONCLUSIONS

A temperature-dependent diffusion regime for xylenes in MIL-47(V) was first evidenced by coupling QENS and MD approaches: (i) a low-temperature regime where the xylene molecules are mainly present close to the pore walls and characterized by a relatively high activation energy for diffusing and (ii) a high-temperature regime where the xylene molecules are situated in the center of the pore with a lower activation energy for diffusing. While the global experimental trend for D_s as a function of the temperature has been very well reproduced by the simulations for all xylenes, they failed to capture the difference in terms of magnitude when one goes from *m*-xylenes to *o*-/*p*-xylenes. This calls for a better description of the host/guest interactions that could be attained by deriving a newly quantum-based force field based on the high-level DFT calculations previously reported in the literature[50] Furthermore, NMR experiments put into evidence that packing effect and guest−guest interactions are crucial when considering dynamics of xylenes confined in MIL-47(V).

AUTHOR INFORMATION

Corresponding Author

*E-mail: herve.jobic@ircelyon.univ-lyon1.fr (H.J.); guillaume.maurin@univ-montp2.fr (G.M.).

Notes

The authors declare no competing financial interest.

ACKNOWLEDGMENTS

We thank the Institut Laue-Langevin for allocating neutron beam time on the IN16 spectrometer. This work was supported by the European Community's Seventh Framework Programme (FP7/2007-2013) under grant agreement no. 228862 and by the Russian Foundation for Basic Research (Grant 13-03-00327). Daniil I. Kolokolov is grateful for support by the Russian Federation Ministry of Education FZP KADRI program.

REFERENCES

(1) Karayannidis, G. P.; Sideridou, I. D.; Zamboulis, D. N.; Bikiaris, D. N.; Sakalis, A. J. Thermal Behavior and Tensile Properties of Poly(ethylene terephthalate-*co*-ethylene isophthalate). *J. Appl. Polym. Sci.* **2000**, *78*, 200−207.

(2) Laurich, S. A. p-Xylene Process. US Patent 3467724, September 16, 1969.

(3) Vicens, J.; Armah, A. E.; Fuji, S.; Tomita, K. I. Separation of Xylenes by Extractive Crystallization with Calixarenes. *J. Inclusion Phenom. Mol. Recognit. Chem.* **1991**, *10*, 159−163.

(4) Shiau, L. D.; Wen, C. C.; Lin, B. S. Separation of *p*-Xylene from the Multicomponent Xylene System by Stripping Crystallization. *AIChE J.* **2008**, *54*, 337−342.

(5) Roesler, C. M.; Kulprathipanja, S.; Rekoske, J. E. Adsorptive Separation Process for Recovery of Para-xylene. US Patent 6706938, March 16, 2004.

(6) Vickers, G. H. Para-xylene and Ethylbenzene Separation from Mixed C8 Aromatics. US Patent 20040010170, January 15, 2004.

(7) Leflaive, P.; Barthelet, K. Process for Separating Meta-xylene from a Feed of Aromatic Hydrocarbons by Liquid Phase Adsorption. US Patent 7468468, December 23, 2008.

(8) Broughton, D. B.; Neuzil, R. W.; Pharis, J. M.; Brearley, C. S. The Parex Process for the Recovery of Paraxylene. *Chem. Eng. Prog.* **1970**, *66*, 70−75.

(9) Minceva, M.; Gomes, P. S.; Meshko, V.; Rodrigues, A. E. Simulated Moving Bed Reactor for Isomerization and Separation of *p*-xylene. *Chem. Eng. J.* **2008**, *140*, 305−323.

(10) Jin, W. H.; Wankat, P. C. Hybrid Simulated Moving Bed Processes for the Purification of *p*-Xylene. *Sep. Sci. Technol.* **2007**, *42*, 669−700.

(11) Minceva, M.; Rodrigues, A. E. Influence of the Transfer Line Dead Volume on the Performance of an Industrial Scale Simulated Moving Bed for *p*-Xylene Separation. *Sep. Sci. Technol.* **2003**, *38*, 1463−1497.

(12) Drechsel, B.; Haêntsch, W.; Weber, K. Contributions for Design and Optimization of Adsorption Processes. Influence of the Adsorber Control. *Chem. Technol.* **1991**, *43*, 57−60.

(13) Spindler, H.; Stief, C.; Haêntsch, W.; Entner, R. The Influence of the Composition of Desorbents on a Number of Sorption Properties of the Ca-exchanged 5A Molecular Sieve in the Parex Process. *Chem. Technol.* **1990**, *42*, 159−160.

(14) Hulme, R.; Rosensweig, R. E.; Ruthven, D. M. Binary and Ternary Equilibria for C_8 Aromatics on K-Y Faujasite. *Ind. Eng. Chem. Res.* **1991**, *30*, 752−760.

(15) Guth, J.-L.; Jacques, P.; Stoessel, F.; Wey, R. On the Thermodynamic Factors Governing the Adsorption of *p*-Xylene and *m*-Xylene onto Faujasite Zeolite Containing Na^+ and K^+ Cations. *J. Colloid Interface Sci.* **1980**, *76*, 298−304.

(16) Daramola, M. O.; Burger, A. J.; Pera-Titus, M.; Giroir-Fendler, A.; Miachon, S. Dalmon, J. A.; Lorenzen, L. Separation and

Isomerization of Xylenes using Zeolite Membranes: a Short Overview. *Asia-Pac. J. Chem. Eng.* **2010**, *5*, 815−837.
(17) Kurup, A. S.; Hidajat, K.; Ray, A. K. Optimal Operation of an Industrial-Scale Parex Process for the Recovery of *p*-Xylene from a Mixture of C_8 Aromatics. *Ind. Eng. Chem. Res.* **2005**, *44*, 5703−5714.
(18) Minceva, M.; Rodrigues, A. E. Adsorption of Xylenes on Faujasite-Type Zeolite: Equilibrium and Kinetics in Batch Adsorber. *Chem. Eng. Res. Des.* **2004**, *82*, 667−681.
(19) Cottier, V.; Bellat, J.-P.; Simonot-Grange, M.-H.; Methivier, A. Adsorption of *p*-Xylene and *m*-Xylene Gas Mixtures on BaY and NaY Zeolites. Coadsorption Equilibria and Selectivities. *J. Phys. Chem. B* **1997**, *101*, 4798−4802.
(20) Roethe, K. P.; Fiedler, K.; Roethe, A.; Suckow, M.; Stach, H.; Spindler, H.; Wittke, H.; Seidel, G.; Ermischer, W.; Roscher, W.; et al. On the Sorption Properties of Na(Ca,Mg) A Molecular Sieves Used in the Parex Process. *Chem. Technol.* **1985**, *37*, 107−112.
(21) Gu, X. H.; Dong, J. H.; Nenoff, T. M.; Ozokwelu, D. E. Separation of *p*-Xylene from Multicomponent Vapor Mixtures Using Tubular MFI Zeolites Membranes. *J. Membr. Sci.* **2006**, *280*, 624−633.
(22) Guo, G. Q.; Chen, H.; Long, Y. C. Separation of *p*-Xylene from C_8 Aromatics on Binder-free Hydrophobic Adsorbent of MFI Zeolite. I. Studies on Static Equilibrium. *Microporous Mesoporous Mater.* **2000**, *39*, 149−161.
(23) Mohammadi, T.; Rezaeian, M. P. Separation of Isomeric Xylenes: Experimental and Modeling. *Sep. Sci. Technol.* **2009**, *44*, 817−840.
(24) Wu, Z. X.; Yang, Y. X.; Tu, B.; Webley, P. A.; Zhao, D. Y. Adsorption of Xylene Isomers on Ordered Hexagonal Mesoporous FDU-15 Polymer and Carbon Materials. *Adsorption* **2009**, *15*, 123−132.
(25) McCandless, F. P.; Downs, W. B. Separation of C_8 Aromatic Isomers by Pervaporation through Commercial Polymer Films. *J. Membr. Sci.* **1987**, *30*, 111−116.
(26) Férey, G. Hybrid Porous Solids; Past, Present, Future. *Chem. Soc. Rev.* **2008**, *37*, 191−214;Metal-Organic Frameworks Editorial. *Chem. Rev.* **2012**, *112*, (2); Metal-Organic Frameworks Editorial. *Chem. Soc. Rev.* **2009**, *38*, 1380−1399.
(27) Li, J.-R.; Sculley, J.; Zhou, H.-C. Metal-Organic Frameworks for Separations. *Chem. Rev.* **2012**, 869−932.
(28) Férey, G.; Serre, C.; Devic, T.; Maurin, G.; Jobic, H.; Llewellyn, P. L.; De Weireld, G.; Vimont, A.; Daturi, M.; Chang, J. S. Why Hybrid Porous Solids Capture Greenhouse Gases? *Chem. Soc. Rev.* **2011**, *40*, 550−562.
(29) Sumida, K.; Rogow, D. L.; Mason, J. A.; McDonald, T. M.; Bloch, E. D.; Herm, Z. R.; Bae, T. H.; Long, J. R. Carbon Dioxide Capture in Metal-Organic Frameworks. *Chem. Rev.* **2012**, *112*, 724−781.
(30) Bloch, E. D.; Queen, W. L.; Krishna, R.; Zadrozny, J. M.; Brown, C. M.; Long, J. R. Hydrocarbons Separations in a Metal-Organic Framework with Open Iron(II) Coordination Sites. *Science* **2012**, *335*, 1606−1610.
(31) Bae, Y. S.; Lee, C. Y.; Kim, K. C.; Farha, O. K.; Nickias, P.; Hupp, J. T.; Nguyen, S. T.; Snurr, R. Q. High Propene/Propane Selectivity in Isostructural Metal-Organic Frameworks with High Densities of Open Metal Sites. *Angew. Chem., Int. Ed.* **2012**, *51*, 1857−1860.
(32) Yoon, J. W.; Seo, Y. K.; Hwang, Y. K.; Chang, J. S.; Leclerc, H.; Wuttke, S.; Bazin, P.; Vimont, A.; Daturi, M.; Bloch, E.; et al. Controlled Reducibility of a Metal-Organic Framework with Coordinatively Unsaturated Sites for Preferential Gas Sorption. *Angew. Chem., Int. Ed.* **2010**, *49*, 5949−5952.
(33) Peralta, D.; Chaplais, G.; Simon-Masseron, A.; Barthelet, K.; Chizallet, C.; Quoineaud, A. A.; Pirngruber, G. D. Comparison of the Behavior of Metal-Organic Frameworks and Zeolites for Hydrocarbons Separations. *J. Am. Chem. Soc.* **2012**, *134*, 8115−81126.
(34) Huang, L. M.; Wang, H. T.; Chen, J. X.; Wang, Z. B.; Sun, J. Y.; Zhao, D. Y.; Yan, Y. S. Synthesis, Morphology Control, and Properties of Porous Metal-Organic Coordination Polymers. *Microporous Mesoporous Mater.* **2003**, *58*, 105−114.
(35) Gu, Z. Y.; Jiang, D. Q.; Wang, H. F.; Cui, X. Y.; Yan, X. P. Adsorption and Separation of Xylene Isomers and Ethylbenzene on Two Zn-Terephthalalte Metal-Organic Frameworks. *J. Phys. Chem. C* **2010**, *114*, 311−316.
(36) Nicolau, M. P. M.; Barcia, P. S.; Gallegos, J. M.; Silva, J. A. C.; Rodrigues, A. E.; Chen, B. L. Single- and Multicomponent Vapor-Phase Adsorption of Xylene Isomers and Ethylbenzene in a Microporous Metal-Organic Framework. *J. Phys. Chem. C* **2009**, *113*, 13173−13179.
(37) Gu, Z.-Y.; Yan, X.-P. Metal-Organic Framework MIL-101 for High-Resolution Gas-Chromatographic Separation of Xylene Isomers and Ethylbenzene. *Angew. Chem., Int. Ed.* **2010**, *49*, 1477−1480.
(38) Jin, Z.; Zhao, H. Y.; Zhao, X. J.; Fang, Q. R.; Long, J. R. A; Zhu, G. S. Novel Microporous MOF with the Capability of Selective Adsorption of Xylenes. *Chem. Commun.* **2010**, *46*, 8612−8614.
(39) Barcia, P. S.; Guimaraes, D.; Mendes, P. A. P.; Silva, J. A. C.; Guillerm, V.; Chevreau, H.; Serre, C.; Rodrigues, A. E. Reverse Shape Selectivity in the Adsorption of Hexane and Xylene Isomers in MOF UiO-66. *Microporous Mesoporous Mater.* **2011**, *139*, 67−73.
(40) Vermoortele, F.; Maes, M.; Moghadam, P. Z.; Lennox, M. J.; Ragon, F.; Boulhout, M.; Biswas, S.; Laurier, K. G. M.; Beurroies, I.; Denoyel, R.; et al. *p*-Xylene-Selective Metal-Organic Frameworks: A Case of Topology-Directed Selectivity. *J. Am. Chem. Soc.* **2011**, *133*, 18526−18529.
(41) Moreira, M. A.; Santos, J. C.; Ferreira, A. F. P.; Loureiro, J. M.; Ragon, F.; Horcajada, P.; Shim, K. E.; Hwang, Y. K.; Lee, U. H.; Chang, J. S.; et al. Reverse Shape Selectivity in the Liquid-Phase Adsorption of Xylene Isomers in Zirconium Terephthalate MOF UiO-66. *Langmuir* **2012**, *28*, 5715−5723.
(42) Finsy, V.; Kirschhock, C. E. A.; Vedts, G.; Maes, M.; Alaerts, L.; De Vos, D. E.; Baron, G. V.; Denayer, J. F. M. Framework Breathing in the Vapour-Phase Adsorption and Separation of Xylene Isomers with the Metal-Organic Framework MIL-53. *Chem.—Eur. J.* **2009**, *15*, 7724−7731.
(43) Moreira, M. A.; Santos, J. C.; Ferreira, A. F. P.; Loureiro, J. M.; Rodrigues, A. E. Influence of the Eluent in the MIL-53(Al) Selectivity for Xylene Isomers Separation. *Ind. Eng. Chem. Res.* **2011**, *50*, 7688−7695.
(44) Moreira, M. A.; Santos, J. C.; Ferreira, A. F. P.; Muller, U.; Trukhan, N.; Loureiro, J. M.; Rodrigues, A. E. Selective Liquid Phase Separation of ortho-Xylene with the Microporous MIL-53(Al). *Sep. Sci. Technol.* **2011**, *46*, 1995−2003.
(45) El Osta, R.; Carlin-Sinclair, A.; Guillou, N.; Walton, R. I.; Vermoortele, F.; Maes, M.; de Vos, D.; Millange, F. Liquid-Phase Adsorption and Separation of Xylene Isomers by the Flexible Porous Metal-Organic Framework MIL-53(Fe). *Chem. Mater.* **2012**, *24*, 2781−2791.
(46) Alaerts, L.; Kirschhock, C. E. A.; Maes, M.; van der Veen, M. A.; Finsy, V.; Depla, A.; Martens, J. A.; Baron, G. V.; Jacobs, P. A.; Denayer, J. E. M.; et al. Selective Adsorption and Separation of Xylene Isomers and Ethylbenzene with the Porous Vanadium(IV) Terephthalate MIL-47. *Angew. Chem., Int. Ed.* **2007**, *46*, 4293−4297.
(47) Finsy, V.; Verelst, H.; Alaerts, L.; De Vos, D.; Jacobs, P. A.; Baron, G. V.; Denayer, J. F. M. Pore-Filling-Dependent Selectivity Effects in the Vapor-Phase Separation of Xylene Isomers on the Metal-Organic Framework MIL-47. *J. Am. Chem. Soc.* **2008**, *130*, 7110−7118.
(48) Maes, M.; Vermoortele, F.; Boulhout, M.; Boudewijns, T.; Kirschhock, C.; Ameloot, R.; Beurroies, I.; Denoyel, R.; De Vos, D. E. Enthalpic Effects in the Adsorption of Alkylaromatics in the Metal-Organic Frameworks MIL-47 and MIL-53. *Microporous Mesoporous Mater.* **2012**, *157*, 82−88.
(49) Castillo, J. M.; Vlugt, T. J. H.; Calero, S. Molecular Simulation Study on the Separation of Xylene Isomers in MIL-47 Metal-Organic Frameworks. *J. Phys. Chem. C* **2009**, *113*, 20869−20874.
(50) Ghysels, A.; Vandichel, M.; Verstraelen, T.; van der Veen, M. A.; De Vos, D. E.; Waroquier, M.; Van Speybroeck, V. Host-Guest and Guest-Guest Interactions between Xylene Isomers Confined in the MIL-47(V) Pore System. *Theor. Chem. Acc.* **2012**, 1234−1246.

(51) Salles, F.; Jobic, H.; Maurin, G.; Koza, M. M.; Llewellyn, P. L.; Devic, T.; Serre, C.; Ferey, G. Experimental Evidence Supported by Simulations of a Very High H_2 Diffusion in Metal Organic Framework Materials. *Phys. Rev. Lett.* **2008**, 245901.1−245901.4.
(52) Salles, F.; Kolokolov, D. I.; Jobic, H.; Maurin, G.; Llewellyn, P. L.; Devic, T.; Serre, C.; Férey, G. Adsorption and Diffusion of H_2 in the MOF Type Systems MIL-47(V) and MIL-53(Cr): A Combination of Microcalorimetry and QENS Experiments with Molecular Simulations. *J. Phys. Chem. C* **2009**, *113*, 7802−7812.
(53) Salles, F.; Jobic, H.; Devic, T.; Llewellyn, P. L.; Serre, C.; Férey, G.; Maurin, G. Self and Transport Diffusivity of CO_2 in the Metal-Organic Framework MIL-47(V) Explored by Quasi-Elastic Neutron Scattering Experiments and Molecular Dynamics Simulations. *ACS Nano* **2010**, *4*, 143−152.
(54) Kolokolov, D. I.; Jobic, H.; Stepanov, A. G.; Ollivier, J.; Rives, S.; Maurin, G.; Devic, T.; Serre, C.; Ferey, G. Experimental and Simulation Evidence of a Corkscrew Motion for Benzene in the Metal-Organic Framework MIL-47. *J. Phys. Chem. C* **2012**, *116*, 15093−15098.
(55) Rosenbach, N.; Jobic, H.; Ghoufi, A.; Salles, F.; Maurin, G.; Bourrelly, S.; Llewellyn, P. L.; Devic, T.; Serre, C.; Férey, G. Quasi-Elastic Neutron Scattering and Molecular Dynamics Study of Methane Diffusion in Metal-Organic Frameworks MIL-47(V) and MIL-53(Cr). *Angew. Chem., Int. Ed.* **2008**, *47*, 6611−6615.
(56) Jobic, H.; Rosenbach, N.; Ghoufi, A.; Kolokolov, D. I.; Yot, P. G.; Devic, T.; Serre, C.; Férey, G.; Maurin, G. Unusual Chain-Length Dependence of the Diffusion of *n*-Alkanes in the Metal-Organic Framework MIL-47(V): The Blowgun Effect. *Chem.—Eur. J.* **2010**, *16*, 10337−10341.
(57) Rives, S.; Jobic, H.; Ragon, F.; Devic, T.; Serre, C.; Ferey, G.; Ollivier, J.; Maurin, G. Diffusion of Long Chain *n*-Alkanes in the Metal-Organic Framework MIL-47(V): A Combination of Neutron Scattering Experiments and Molecular Dynamics Simulations. *Microporous Mesoporous Mater.* **2012**, *164*, 259−265.
(58) Salles, F.; Jobic, H.; Ghoufi, A.; Llewellyn, P. L.; Serre, C.; Bourrelly, S.; Ferey, G.; Maurin, G. Transport Diffusivity of CO_2 in the Highly Flexible Metal-Organic Framework MIL-53(Cr). *Angew. Chem., Int. Ed.* **2009**, *48*, 8335−8339.
(59) Salles, F.; Bourrelly, S.; Jobic, H.; Devic, T.; Guillerm, V.; Llewellyn, P.; Serre, C.; Ferey, G.; Maurin, G. Molecular Insight into the Adsorption and Diffusion of Water in the Versatile Hydrophilic/Hydrophobic Flexible MIL-53(Cr) MOF. *J. Phys. Chem. C* **2011**, *115*, 10764−10776.
(60) Yang, Q. Y.; Wiersum, A. D.; Jobic, H.; Guillerm, V.; Serre, C.; Llewellyn, P. L.; Maurin, G. Understanding the Thermodynamic and Kinetic Behavior of the CO_2/CH_4 Gas Mixture within the Porous Zirconium Terephthalate UiO-66(Zr): A Joint Experimental and Modeling Approach. *J. Phys. Chem. C* **2011**, *115*, 13768−13774.
(61) Yang, Q. Y.; Jobic, H.; Salles, F.; Kolokolov, D.; Guillerm, V.; Serre, C.; Maurin, G. Probing the Dynamics of CO_2 and CH4 within the Porous Zirconium Terephthalate UiO-66(Zr). *Chem.—Eur. J.* **2011**, *17*, 8882−8889.
(62) Mizuno, M.; Itakura, N.; Endo, K. Effects of Strong Paramagnetic Interactions on Solid-State Deuterium NMR Spectra. *Chem. Phys. Lett.* **2005**, *416*, 358−363.
(63) Barthelet, K.; Marrot, J.; Riou, D.; Ferey, G. A Breathing Hybrid Organic-Inorganic Solid with Very Large Pores and High Magnetic Characteristics. *Angew. Chem., Int. Ed.* **2001**, *41*, 281−284.
(64) Antonijevic, S.; Wimperis, S. Refocussing of Chemical and Paramagnetic Shift Anisotropies in $_2$H NMR Using the Quadrupole-Echo Experiment. *J. Magn. Reson.* **2003**, *164*, 343−350.
(65) Trung, T. K.; Deroche, I.; Rivera, A.; Yang, Q. Y.; Yot, P.; Ramsahye, N.; Vinot, S. D.; Devic, T.; Horcajada, P.; Serre, C.; et al. Hydrocarbon Adsorption in the Isostructural Metal-Organic Frameworks MIL-53(Cr) and MIL-47(V). *Microporous Mesoporous Mater.* **2011**, *140*, 114−119.
(66) Kolokolov, D. I.; Jobic, H.; Stepanov, A. G.; Guillerm, V.; Devic, T.; Serre, C.; Férey, G. Dynamics of Benzene Rings in MIL-53(Cr) and MIL-47(V) Frameworks Studied by ^{2}H NMR Spectroscopy. *Angew. Chem., Int. Ed.* **2010**, *49*, 4791−4794.
(67) Yot, P. G.; Ma, Q. T.; Haines, J.; Yang, Q. Y.; Ghoufi, A.; Devic, T.; Serre, C.; Dmitriev, V.; Férey, G.; Zhong, C. L.; et al. Large Breathing of the MOF MIL-47(V) under Mechanical Pressure: a Joint Experimental-Modeling Exploration. *Chem. Sci.* **2012**, *3*, 1100−1104.
(68) Ramsahye, N. A.; Maurin, G.; Bourrelly, S.; Llewellyn, P.; Loiseau, T.; Férey, G. Charge Distribution in Metal Organic Framework Materials: Transferability to a Preliminary Molecular Simulation Study of CO_2 adsorption in the MIL-53(Al) System. *Phys. Chem. Chem. Phys.* **2007**, *9*, 1059−1063.
(69) Rappe, A. K.; Casewit, C. J.; Colwell, K. S.; Goddard, W. A.; Skiff, W. M. UFF, a Full Periodic Table Force Field for Molecular Mechanics and Molecular Dynamics Simulations. *J. Am. Chem. Soc.* **1992**, *114*, 10024−10035.
(70) Mayo, S. L.; Olafson, B. D.; Goddard, W. A. DREIDING: a Generic Force Field for Molecular Simulations. *J. Phys. Chem.* **1990**, *94*, 8897−8909.
(71) Rai, N.; Siepmann, J. I. Transferable Potentials for Phase Equilibria. 9. Explicit Hydrogen Description of Benzene and Five-Membered and Six-Membered Heterocyclic Aromatic Compounds. *J. Phys. Chem. B* **2007**, *111*, 10790−10799.
(72) Wick, C. D.; Martin, M. G.; Siepmann, J. I. Transferable Potentials for Phase Equilibria. 4. United-Atom Description of Linear and Branched Alkenes and of Alkylbenzenes. *J. Phys. Chem. B* **2000**, *104*, 8008−8016.
(73) Oie, T.; Maggiora, G. M.; Christoffersen, R. E.; Duchamp, D. J. Development of a Flexible Intra- and Intermolecular Empirical Potential Function for Large Molecular Systems. *Int. J. Quantum Chem.* **1981**, *20*, 1−47.
(74) Smith, W.; Forester, T. R. DL-POLY-2.0: A General-Purpose Parallell Molecular Dynamics Simulation Package. *J. Mol. Graphics* **1996**, *14*, 136−141.
(75) Frenkel, D.; Smit, B. *Understanding Molecular Simulation*; Academic Press: New York, 1996.
(76) Beerdsen, E.; Smit, B.; Dubbeldam, D. Molecular Simulation of Loading Dependent Slow Diffusion in Confined Systems. *Phys. Rev. Lett.* **2004**, *93*, 248301.1−248301.4.
(77) Jobic, H.; Bée, M.; Méthivier, A.; Combet, J. Influence of the Cation Composition on the Dynamics of Xylenes in X-type Zeolites. *Microporous Mesoporous Mater.* **2001**, *42*, 135−155.
(78) Zhai, D.; Zhao, L.; Gao, J. S.; Xu, C. M. Effect of Temperature on the Diffusion Mechanism of Xylene Isomers in a FAU zeolite: a Molecular Dynamics Study. *Phys. Chem. Chem. Phys.* **2012**, *14*, 7296−7303.
(79) Takakura, K.; Ueda, T.; Miyakubo, K.; Eguchi, T. Local Structure and Dynamics of Benzene Confined in the IRMOF-1 Nanocavity as Studied by Molecular Dynamics Simulation. *Phys. Chem. Chem. Phys.* **2013**, *15*, 279−290.
(80) Krishna, R.; Li, S.; van Baten, J. M.; Falconer, J. L.; Noble, R. D. Investigation of Slowing-down and Speeding-up Effects in Binary Mixture Permeation across SAPO-34 and MFI Membranes. *Sep. Purif. Technol.* **2008**, *60*, 230−236.
(81) Krishna, R. Diffusion in Porous Crystalline Materials. *Chem. Soc. Rev.* **2012**, *41*, 3099−3118.
(82) Jelinski, L. W. In *High Resolution NMR Spectroscopy of Synthetic Polymers in Bulk (Methods and Stereochemical Analysis)*; Komoroski, R. A., Ed.; VCH Publishers: New York, 1986; Vol. 7, p 335.
(83) Geil, B.; Isfort, O.; Boddenberg, B.; Favre, D. E.; Chmelka, B. F.; Fujara, F. Reorientational and Translational Dynamics of Benzene in Zeolite NaY as Studied by One- and Two-Dimensional Exchange Spectroscopy and Static-Field-Gradient Nuclear Magnetic Resonance. *J. Chem. Phys.* **2002**, *116*, 2184−2193.
(84) Spiess, H. W. In *NMR Basic Principles and Progress*; Diehl, P., Fluck, E., Kosfeld, R., Eds.; Springer-Verlag: New York, 1978; Vol. *15*, p 55.
(85) Macho, V.; Brombacher, L.; Spiess, H. W. The NMR-WEBLAB: An Internet Approach to NMR Lineshape Analysis. *Appl. Magn. Reson.* **2001**, *20*, 405−432.